

Large electroweak corrections to vector-boson scattering at the Large Hadron Collider

Benedikt Biedermann,¹ Ansgar Denner,¹ and Mathieu Pellen¹

¹Universität Würzburg, Institut für Theoretische Physik und Astrophysik, D-97074 Würzburg, Germany

(Dated: June 16, 2017)

For the first time full next-to-leading-order electroweak corrections to off-shell vector-boson scattering are presented. The computation features the complete matrix elements, including all non-resonant and off-shell contributions, to the electroweak process $pp \rightarrow \mu^+\nu_\mu e^+\nu_e jj$ and is fully differential. We find surprisingly large corrections, reaching -16% for the fiducial cross section, as an intrinsic feature of vector-boson-scattering processes. We elucidate the origin of these large electroweak corrections upon using the double-pole approximation and the effective vector-boson approximation along with leading-logarithmic corrections.

PACS numbers: 12.15.Ji, 12.15.Lk, 13.40.Ks, 11.15.Ex

Introduction

Since the Higgs boson has been discovered at the Large Hadron Collider (LHC), a significant experimental program has been devoted to the study of the electroweak (EW) sector of the Standard Model [1]. The Higgs boson plays a crucial role in vector-boson scattering (VBS) as it prevents the amplitude from violating unitarity at high energies. VBS is thus a basic process to investigate the mechanism of EW symmetry breaking. In addition, VBS is a key testing ground for possible new interactions, as it is particularly sensitive to small deviations from the Standard Model, which can, for example, be parametrized by anomalous quartic gauge-boson couplings. Hence, precise predictions for this process will allow one to impose more stringent exclusion limits on new physics models or even trigger the discovery of new fundamental mechanisms.

VBS at the LHC is an exclusive process where a constituent of each colliding proton emits a weak vector boson $V = W, Z$ which then scatter off each other. The emissions from the protons cause jets in the forward and backward directions with large rapidity difference and dijet invariant mass. The resulting $VVjj$ final state receives contributions from both EW and QCD mediated processes, referred to as EW and strong production that can be separated in a gauge-invariant way. Strong production can be suppressed by requiring the above-mentioned tagging jets in the forward and backward directions. In the following, we refer to the EW production mode of the $VVjj$ final state as the actual VBS process.

The present letter focuses on the EW production of two off-shell W^+ bosons in association with two jets, *i.e.* $pp \rightarrow \mu^+\nu_\mu e^+\nu_e jj$, which has been identified as the most promising channel for the measurement of VBS [2] at the LHC. For like-sign WW scattering, the strong production mode does not dominate over the EW mode, in contrast to most other VBS processes. Evidence for this process has already been reported by both the ATLAS [3, 4] and CMS [5] collaborations.

Significant interest has been devoted in the past to the computation of higher-order corrections to VBS and

its main irreducible background processes [6–13]. So far, these computations have focused exclusively on next-to-leading-order (NLO) QCD corrections, and no NLO EW computation has been performed yet. As the impact of EW corrections grows with the energy owing to the presence of logarithms of the ratio of energy and EW gauge-boson mass, so-called Sudakov logarithms, they have to be calculated in view of the increasing energy and luminosity of the LHC. In this letter we present first results for the full NLO EW corrections to the off-shell VBS process $pp \rightarrow \mu^+\nu_\mu e^+\nu_e jj$.

The EW corrections to the integrated cross section turn out to be surprisingly large compared to those for other standard LHC processes. In order to elucidate the origin of these enhanced corrections, we study results for EW corrections also in two approximations, the double-pole approximation and the effective vector-boson approximation (EVBA). Our results allow one to include these corrections in precise measurements of VBS at the LHC.

Details of the calculation

We consider the leading-order EW process $pp \rightarrow \mu^+\nu_\mu e^+\nu_e jj$ of order $\mathcal{O}(\alpha^6)$. The dominant partonic channel $uu \rightarrow \mu^+\nu_\mu e^+\nu_e dd$ accounts for about two thirds of the cross section. The second largest channel $u\bar{d} \rightarrow \mu^+\nu_\mu e^+\nu_e d\bar{u}$ features a Higgs boson in the s channel and makes up 16% of the cross section. The remaining partonic channels sum up to 17% of the cross section. The EW NLO corrections comprise all contributions of order $\mathcal{O}(\alpha^7)$. These include the complete EW virtual one-loop amplitude and real photon radiation, *i.e.* the process $pp \rightarrow \mu^+\nu_\mu e^+\nu_e jj\gamma$. At order $\mathcal{O}(\alpha^7)$, also contributions of the type $q_1\gamma \rightarrow \mu^+\nu_\mu e^+\nu_e q_2 q_3 \bar{q}_4$ appear, where q_i are quarks of possibly different type. These real corrections are suppressed owing to the photon distribution function and therefore have been omitted in the present computation.

The resonant particles are treated within the complex-

mass scheme [14, 15], ensuring gauge invariance. To evaluate all one-loop amplitudes in the 6-body phase space, the computer code RECOLA [16, 17] and the COLLIER library [18, 19] are employed. The phase-space integration is carried out with two different Monte Carlo programs that have been used in Refs. [20, 21] and Refs. [22, 23], respectively. The infrared singularities are treated via the Catani–Seymour dipole subtraction formalism [24, 25]. The collinear initial-state splittings are handled within the DIS factorization scheme following Refs. [26, 27].

To ensure the correctness of the results, a number of checks has been performed. We have verified numerically that the sum of all corrections is infrared finite. The hadronic Born cross section has been compared against the computer code MADGRAPH5_AMC@NLO [28], which has also been used to check the tree-level matrix elements squared (for Born and real radiation). Finally, for the dominant partonic channels (uu and $u\bar{d}$) a computation in the double-pole approximation (based on an automatized implementation following the one of Ref. [23]) has confirmed the NLO EW corrections obtained in the full calculation within an accuracy below 1%.

Input parameters and event selections

We present theoretical predictions for the LHC at the center-of-mass energy of 13 TeV. The on-shell values for the masses and widths of the gauge bosons

$$\begin{aligned} M_W^{\text{os}} &= 80.385 \text{ GeV}, & \Gamma_W^{\text{os}} &= 2.085 \text{ GeV}, \\ M_Z^{\text{os}} &= 91.1876 \text{ GeV}, & \Gamma_Z^{\text{os}} &= 2.4952 \text{ GeV} \end{aligned} \quad (1)$$

are converted into pole masses according to

$$\begin{aligned} M_V &= M_V^{\text{os}}/c_V, & \Gamma_V &= \Gamma_V^{\text{os}}/c_V, \\ c_V &= \sqrt{1 + (\Gamma_V^{\text{os}}/M_V^{\text{os}})^2}, & V &= W, Z. \end{aligned} \quad (2)$$

The Higgs-boson and top-quark masses and widths are fixed to

$$\begin{aligned} M_H &= 125 \text{ GeV}, & \Gamma_H &= 4.07 \times 10^{-3} \text{ GeV}, \\ m_t &= 173.21 \text{ GeV}, & \Gamma_t &= 0 \text{ GeV}. \end{aligned}$$

The top-quark width can be neglected since no resonant top quarks appear in the matrix elements.

For the electromagnetic coupling α , the G_μ scheme is used where α is obtained from the Fermi constant,

$$\alpha_{G_\mu} = \sqrt{2}G_\mu M_W^2 (1 - M_W^2/M_Z^2) / \pi, \quad (3)$$

with

$$G_\mu = 1.16637 \times 10^{-5} \text{ GeV}^{-2}. \quad (4)$$

We have chosen the set of parton distribution functions NNPDF3.0QED [29, 30]. The renormalization and factorization scales, μ_{ren} and μ_{fact} , are set equal to the pole mass of the W boson, $\mu_{\text{ren}} = \mu_{\text{fact}} = M_W$.

σ^{LO} [fb]	$\sigma_{\text{EW}}^{\text{NLO}}$ [fb]	δ_{EW} [%]
1.5348(2)	1.2895(6)	-16.0

TABLE I: LO and NLO cross section for $pp \rightarrow \mu^+ \nu_\mu e^+ \nu_e jj$ at 13 TeV at the LHC. The corresponding EW corrections are given in per cent. The digit in parenthesis indicates the integration error.

The event selection for VBS is based on the experimental analyses of ATLAS [3] and CMS [5]. Quarks and gluons are clustered using the anti- k_T algorithm [31] with jet-resolution parameter $R = 0.4$. The recombination of photons with charged particles employs a resolution parameter $R = 0.1$.

For each jet and charged lepton, a cut on its transverse momentum and its rapidity is applied,

$$p_{T,j} > 30 \text{ GeV}, \quad |y_j| < 4.5, \quad (5)$$

$$p_{T,\ell} > 20 \text{ GeV}, \quad |y_\ell| < 2.5, \quad (6)$$

and the missing energy has to fulfill

$$E_T^{\text{miss}} > 40 \text{ GeV}. \quad (7)$$

For the pair of jets, an invariant mass cut and a cut on the difference of the rapidities is applied,

$$M_{jj} > 500 \text{ GeV}, \quad |\Delta y_{jj}| > 2.5. \quad (8)$$

Finally, the leptons are required to be isolated,

$$\Delta R_{\ell\ell} > 0.3, \quad \Delta R_{j\ell} > 0.3, \quad (9)$$

where

$$\Delta R_{ij} = \sqrt{(\Delta y_{ij})^2 + (\Delta \phi_{ij})^2} \quad (10)$$

is the rapidity–azimuthal-angle distance of the objects i and j .

Numerical results

The fiducial cross section for the VBS event selection (5)–(9) and the corresponding NLO EW corrections are reported in Table I. Strikingly, the EW corrections turn out to be -16% and thus surprisingly large for a fiducial cross section. For typical LHC processes, such large negative corrections originating from Sudakov logarithms generically show up in the high-energy tails of distributions which usually do not dominate the integrated cross section.

Moreover, these large corrections are not due to the VBS event selections described above but are intrinsic to the VBS process at the LHC [41]. Indeed, dropping the cuts (8) on the two jets and on the missing energy (7) and

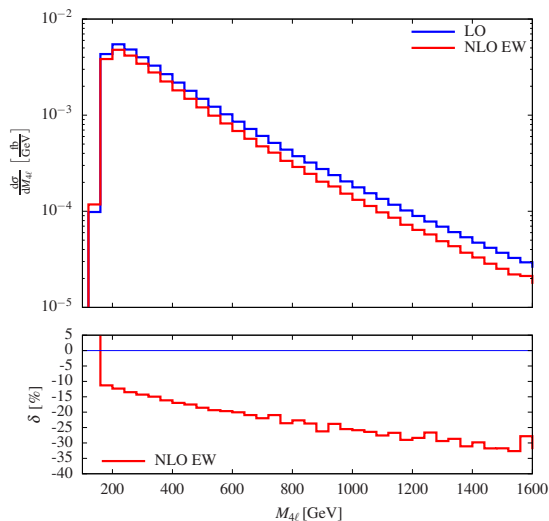


FIG. 1: Invariant-mass distribution of the four leptons in $pp \rightarrow \mu^+ \nu_\mu e^+ \nu_e jj$ including NLO EW corrections (upper panel) and relative NLO EW corrections (lower panel).

relaxing the requirements on the transverse momenta (5) and (6) leave the corrections at the same level.

In Fig. 1, the distribution in the invariant mass of the four leptons is displayed. The upper panel shows the LO and NLO EW prediction and the lower panel the relative EW corrections $\delta = \sigma_{\text{NLO EW}}/\sigma_{\text{LO}} - 1$ in per cent. The cross section drops by one order of magnitude only 500 GeV above its maximum. For typical gauge-boson pair production processes like WW or ZZ production the cross section decreases more than twice as fast with increasing energy. The negative EW corrections increase from -12% at 150 GeV to -32% at 1.6 TeV.

In Fig. 2, the rapidity distribution of the dijet system is presented. In VBS the two jets are typically back to back, and their joint rapidity tends to be close to zero. Near $y_{j_1 j_2} = 0$, the EW corrections are maximal and at the level of -16% as for the integrated cross section. For large $|y_{j_1 j_2}|$ the two jets tend to be in the same hemisphere, and the kinematics is different from the one of VBS. In this kinematic region, the EW corrections turn out to be smaller. The variation of the EW corrections is weaker in other rapidity distributions of the jets and practically absent in those of the leptons.

In addition to the relative corrections, in the lower panel also the expected statistical experimental uncertainty is displayed. Here we assume 3000 fb^{-1} which is the target for a high-luminosity LHC. For each bin we have computed the number of expected events N_{obs} and the corresponding relative uncertainty as $\pm 1/\sqrt{N_{\text{obs}}}$ in per cent which is represented by the band. This clearly demonstrates that the EW corrections are mandatory to describe VBS with sufficient precision at a high luminosity LHC. Note that the expected statistical experimental

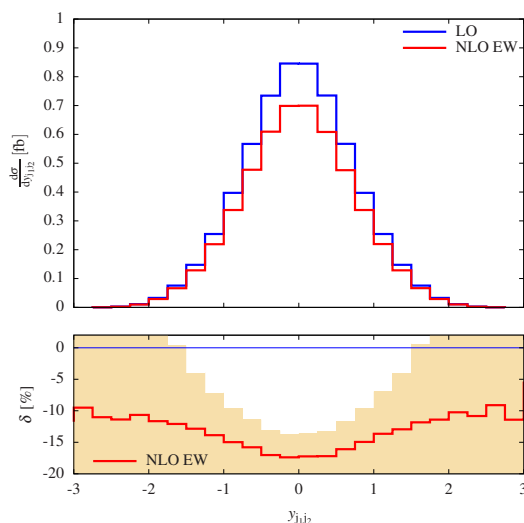


FIG. 2: Rapidity distribution of the leading jet pair in $pp \rightarrow \mu^+ \nu_\mu e^+ \nu_e jj$ including NLO EW corrections (upper panel) and relative NLO EW corrections (lower panel). The yellow band describes the expected statistical experimental uncertainty for a high-luminosity LHC collecting 3000 fb^{-1} and represents a relative variation of $\pm 1/\sqrt{N_{\text{obs}}}$ where N_{obs} is the number of observed events in each bin.

uncertainty for the total cross section is 1.6%.

We follow the experimental analysis and do not include real radiation of W and Z bosons. Including these contributions with realistic experimental cuts would only partially compensate the virtual corrections [32] and even a fully inclusive treatment of massive gauge-boson radiation would not yield a complete cancellation of the Sudakov logarithms [33].

Origin of large electroweak corrections

Upon splitting the EW corrections into the gauge-invariant subsets of fermionic and bosonic parts, we could attribute the large effects exclusively to the bosonic sector. We have furthermore verified at the level of distributions that the leading behavior of the NLO EW corrections is dominated by the virtual corrections. In order to get a feeling for the relevant scales in the process, we calculated the average partonic center-of-mass energy, the average invariant mass of the jet pair, and the average invariant mass of the four-lepton system and found $\langle \sqrt{\hat{s}} \rangle \sim 2.2 \text{ TeV}$, $\langle m_{jj} \rangle \sim 1.6 \text{ TeV}$, and $\langle m_{4\ell} \rangle \sim 390 \text{ GeV}$, respectively.

In view of the complexity of the VBS process and the appearance of many different scales, the study of approximations is useful in order to understand the origin of the large corrections.

As a first step, we have evaluated the subtracted virtual corrections to the VBS process in the double-pole

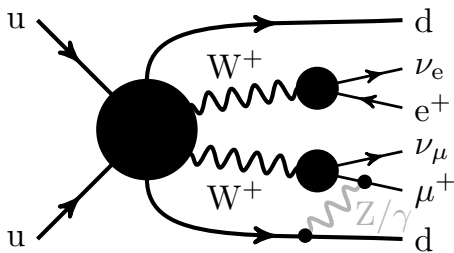


FIG. 3: Schematic representation of the double-pole approximation for the VBS process. The black blobs represent the factorized subprocesses while the grey gauge boson represents a non-factorizable correction.

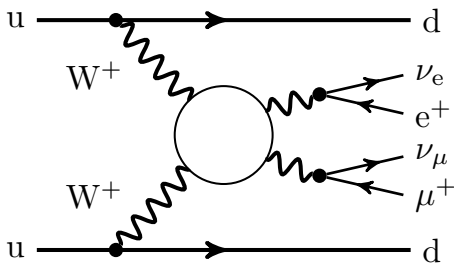


FIG. 4: Schematic representation of the EVBA. The white blob represents the VBS subprocess.

approximation (DPA) [23, 34]. In the DPA two on-shell W bosons are requested, and the matrix elements are split into those for production and decay of the resonant W bosons. This is illustrated in Fig. 3 where the blobs represent the production and decay processes of the W bosons including the factorizable corrections, while the explicit neutral gauge boson (Z, γ) constitutes a typical non-factorizable correction in this framework. We found that the DPA reproduces the full process within 1% and thus provides a sufficiently good approximation for practical purposes. In the DPA, the factorizable corrections constitute $\sim 95\%$ of the subtracted virtual corrections and are thus responsible for the large EW corrections. Moreover, the non-factorizable corrections result exclusively from photon exchange and are compensated upon adding the corresponding real photonic corrections.

To further simplify the discussion, we use the EVBA, depicted schematically in Fig. 4, where two W bosons are radiated off the quark lines to scatter. In this picture, most of the energy is transferred to the two back-to-back jets while the rest of the energy goes into the scattering of the two W bosons in the central region. The invariant masses of the radiated W bosons are space-like but of the order of the W-boson mass to enhance the cross section [13, 35, 36]. While the EVBA constitutes a crude approximation valid only in the very-high-energy limit [36, 37], it is sufficient to discuss the origin of the enhanced EW corrections.

To proceed, we combine the EVBA with the Sudakov approximation in a similar way as pioneered in Ref. [37]

for VBS in electron-positron annihilation. In the Sudakov limit, where all invariants are large, the dominant EW corrections result from double and single logarithms involving ratios of the large invariants and the vector-boson masses squared [38, 39]. In the EVBA the large logarithms in the factorizable corrections result only from the vector-boson-scattering subprocess, $W^+W^+ \rightarrow W^+W^+$. To keep things simple, we only consider the double EW logarithms, the collinear single EW logarithms, and the single logarithms resulting from parameter renormalization. Following Ref. [39], we obtain

$$\sigma_{\text{LL}} = \sigma_{\text{LO}} \left[1 - \frac{\alpha}{4\pi} 4C_{\text{W}}^{\text{ew}} \log^2 \left(\frac{Q^2}{M_{\text{W}}^2} \right) + \frac{\alpha}{4\pi} 2b_{\text{W}}^{\text{ew}} \log \left(\frac{Q^2}{M_{\text{W}}^2} \right) \right], \quad (11)$$

where the EW Casimir operator and the β -function coefficient for W bosons read

$$C_{\text{W}}^{\text{ew}} = \frac{2}{s_{\text{w}}^2}, \quad b_{\text{W}}^{\text{ew}} = \frac{19}{6s_{\text{w}}^2} \quad (12)$$

with the sine of the weak mixing angle s_{w} . Using $\langle m_{4\ell} \rangle \sim 390$ GeV as a typical scale Q for the VBS subprocess leads to an EW correction of about -16% . Applying this logarithmic approximation differentially to the distribution in the invariant mass of the four leptons yields about -15% . These numbers reproduce remarkably well the full correction of -16% given the fact that they include only logarithmic corrections resulting from the VBS subprocess, neglecting even the angular-dependent leading logarithms.

The resulting EW corrections are by a factor of 3–4 larger compared to processes like vector-boson pair production or top-quark pair production for the following reasons. First, the EW Casimir operator C^{ew} is larger for vector bosons than for fermions. This enhances the double logarithmic corrections by a factor of 1.5 for $WW \rightarrow WW$ with respect to $q\bar{q} \rightarrow WW$. Second, the typical scale of the hard scattering process Q is larger for $WW \rightarrow WW$. For a typical pair-production process the scale is more or less of the order of the pair production threshold, *i.e.* $Q \sim 250$ GeV for $q\bar{q} \rightarrow WW/ZZ$, since the cross sections drop with $1/\hat{s}$ above threshold. For $WW \rightarrow WW$, on the other hand, the cross section drops much slower (*c.f.* Fig. 1) owing to the massive t -channel vector-boson exchange in these processes [40]. Without cuts, the cross section would even approach a constant for high energies. The scale $Q = \langle m_{4\ell} \rangle \sim 390$ GeV enhances the double logarithmic corrections by a factor of 1.9 with respect to a scale $Q \sim 250$ GeV. Third, the cancellation between single and double logarithms is weaker for external vector bosons than for external fermions.

Summary

In summary, the NLO EW corrections to a VBS process have been presented for the first time. The fully differential computation includes the full EW NLO matrix elements with all non-resonant and off-shell contributions and can be well reproduced by a double-pole approximation. The EW corrections to the fiducial cross section are with -16% surprisingly large and are an intrinsic feature of VBS. Using the effective vector-boson approximation combined with a high-energy logarithmic approximation for the EW corrections, we have been able to identify the source of these large corrections. They result from large logarithms in the virtual EW corrections to the VBS subprocess. They are enhanced with respect to other LHC processes owing to the comparably large couplings of the vector bosons, reduced cancellations within the logarithmic corrections, and the massive t -channel vector-boson exchange contributions in VBS, which lead to sizeable contributions at large scales. The large EW corrections presented here should be included in any precise analysis of VBS.

Acknowledgements

We thank Jean-Nicolas Lang for providing a version of RECOLA featuring only fermionic corrections and Mauro Chiesa for useful discussions. We acknowledge support by the German Federal Ministry for Education and Research (BMBF) under contract no. 05H15WWCA1 and the German Science Foundation (DFG) under reference number DE 623/6-1.

-
- [1] D. R. Green, P. Meade, and M.-A. Pleier (2016), 1610.07572.
 - [2] J. M. Campbell and R. K. Ellis, *JHEP* **04**, 030 (2015), 1502.02990.
 - [3] G. Aad et al. (ATLAS), *Phys. Rev. Lett.* **113**, 141803 (2014), 1405.6241.
 - [4] M. Aaboud et al. (ATLAS) (2016), 1611.02428.
 - [5] V. Khachatryan et al. (CMS), *Phys. Rev. Lett.* **114**, 051801 (2015), 1410.6315.
 - [6] T. Melia, K. Melnikov, R. Rötsch, and G. Zanderighi, *JHEP* **12**, 053 (2010), 1007.5313.
 - [7] T. Melia, K. Melnikov, R. Rötsch, and G. Zanderighi, *Phys. Rev.* **D83**, 114043 (2011), 1104.2327.
 - [8] B. Jäger, C. Oleari, and D. Zeppenfeld, *Phys. Rev.* **D80**, 034022 (2009), 0907.0580.
 - [9] B. Jäger and G. Zanderighi, *JHEP* **11**, 055 (2011), 1108.0864.
 - [10] A. Denner, L. Hošeková, and S. Kallweit, *Phys. Rev.* **D86**, 114014 (2012), 1209.2389.
 - [11] F. Campanario, M. Kerner, L. D. Ninh, and D. Zeppenfeld, *Phys. Rev.* **D89**, 054009 (2014), 1311.6738.
 - [12] J. Baglio et al. (2014), 1404.3940.
 - [13] M. Rauch (2016), 1610.08420.
 - [14] A. Denner et al., *Nucl. Phys.* **B560**, 33 (1999), hep-ph/9904472.
 - [15] A. Denner et al., *Nucl. Phys.* **B724**, 247 (2005), hep-ph/0505042.
 - [16] S. Actis et al., *JHEP* **04**, 037 (2013), 1211.6316.
 - [17] S. Actis et al., *Comput. Phys. Commun.* **214**, 140 (2017), 1605.01090.
 - [18] A. Denner, S. Dittmaier, and L. Hofer, *PoS* **LL2014**, 071 (2014), 1407.0087.
 - [19] A. Denner, S. Dittmaier, and L. Hofer, *Comput. Phys. Commun.* **212**, 220 (2017), 1604.06792.
 - [20] B. Biedermann, A. Denner, S. Dittmaier, L. Hofer, and B. Jäger, *Phys. Rev. Lett.* **116**, 161803 (2016), 1601.07787.
 - [21] B. Biedermann et al., *JHEP* **06**, 065 (2016), 1605.03419.
 - [22] A. Denner and R. Feger, *JHEP* **11**, 209 (2015), 1506.07448.
 - [23] A. Denner and M. Pellen, *JHEP* **08**, 155 (2016), 1607.05571.
 - [24] S. Catani and M. H. Seymour, *Nucl. Phys.* **B485**, 291 (1997), [Erratum: *Nucl. Phys.* **B510** (1998) 503], hep-ph/9605323.
 - [25] S. Dittmaier, *Nucl. Phys.* **B565**, 69 (2000), hep-ph/9904440.
 - [26] K. P. O. Diener, S. Dittmaier, and W. Hollik, *Phys. Rev.* **D72**, 093002 (2005), hep-ph/0509084.
 - [27] S. Dittmaier and M. Huber, *JHEP* **01**, 060 (2010), 0911.2329.
 - [28] J. Alwall et al., *JHEP* **07**, 079 (2014), 1405.0301.
 - [29] R. D. Ball et al. (NNPDF), *Nucl. Phys.* **B877**, 290 (2013), 1308.0598.
 - [30] R. D. Ball et al. (NNPDF), *JHEP* **04**, 040 (2015), 1410.8849.
 - [31] M. Cacciari, G. P. Salam, and G. Soyez, *JHEP* **04**, 063 (2008), 0802.1189.
 - [32] U. Baur, *Phys. Rev.* **D75**, 013005 (2007), hep-ph/0611241.
 - [33] M. Ciafaloni, P. Ciafaloni, and D. Comelli, *Phys. Rev. Lett.* **87**, 211802 (2001), hep-ph/0103315.
 - [34] S. Dittmaier and C. Schwan, *Eur. Phys. J.* **C76**, 144 (2016), 1511.01698.
 - [35] G. Altarelli, B. Mele, and F. Pitolli, *Nucl. Phys.* **B287**, 205 (1987).
 - [36] I. Kuss and H. Spiesberger, *Phys. Rev.* **D53**, 6078 (1996), hep-ph/9507204.
 - [37] E. Accomando, A. Denner, and S. Pozzorini, *JHEP* **03**, 078 (2007), hep-ph/0611289.
 - [38] P. Ciafaloni and D. Comelli, *Phys. Lett.* **B446**, 278 (1999), hep-ph/9809321.
 - [39] A. Denner and S. Pozzorini, *Eur. Phys. J.* **C18**, 461 (2001), hep-ph/0010201.
 - [40] A. Denner and T. Hahn, *Nucl. Phys.* **B525**, 27 (1998), hep-ph/9711302.
 - [41] Even for a center-of-mass energy of $\sqrt{s} = 7$ TeV we find EW corrections of -13% for the dominating channels.